Biallelic Mutations in *PATL2* Cause Female Infertility Characterized by Oocyte Maturation Arrest

Biaobang Chen,[1,2,7] Zhihua Zhang,[1,7] Xiaoxi Sun,[3,7] Yanping Kuang,[4,7] Xiaoyan Mao,[4,7] Xueqian Wang,[1,7] Zheng Yan,[4] Bin Li,[4] Yao Xu,[1] Min Yu,[3] Jing Fu,[3] Jian Mu,[1] Zhou Zhou,[1] Qiaoli Li,[1] Li Jin,[1] Lin He,[5,6] Qing Sang,[1,2,*] and Lei Wang[1,2,*]

Oocyte maturation arrest results in female infertility, but the genetic determinants of human oocyte maturation arrest remain largely unknown. Previously, we identified *TUBB8* mutations responsible for human oocyte maturation arrest, indicating the important role of genetic factors in the disorder. However, *TUBB8* mutations account for only around 30% of individuals with oocyte maturation arrest; thus, the disorder is likely to involve other genetic factors that are as yet unknown. Here, we initially identified a homozygous nonsense mutation of *PATL2* (c.784C>T [p.Arg262*]) in a consanguineous family with a phenotype characterized by human oocyte germinal vesicle (GV) arrest. Subsequent mutation screening of *PATL2* in a cohort of 179 individuals identified four additional independent individuals with compound-heterozygous *PATL2* mutations with slight phenotypic variability. A genetic burden test further confirmed the genetic contribution of *PATL2* to human oocyte maturation arrest. By western blot in HeLa cells, identification of splicing events in affected individuals' granulosa cells, and immunostaining in affected individuals' oocytes, we provide evidence that mutations in *PATL2* lead to decreased amounts of protein. These findings suggest an important role for *PATL2* mutations in oocyte maturation arrest and expand our understanding of the genetic basis of female infertility.

Successful fertilization in humans requires the fusion of a sperm with a mature oocyte. Oocyte maturation occurs through a series of molecular and morphological changes. Oocytes are initially arrested at the diplotene stage of prophase I, at which point they are referred to as germinal vesicle (GV) oocytes. Upon a surge in luteinizing hormone, GV oocytes exit prophase I and resume meiosis, and this is followed by chromatin condensation and breakdown of the nuclear envelope.[1] Coupled with spindle formation and chromosome alignment, oocytes enter into meiosis I (when they are referred to as MI oocytes). MI is completed by extrusion of the first polar body. Oocytes then enter into meiosis II (when they are referred to as MII oocytes) but arrest at metaphase of MII until fertilization.[2] In clinical *in vitro* fertilization (IVF) and intracytoplasmic sperm injection (ICSI), first polar body (PB1) oocytes are regarded as indicative of MII oocytes, which can be used for fertilization. Oocyte maturation arrest occurs at different stages, including the GV stage and MI, leading to female infertility.[3]

Human oocyte maturation arrest was first described in 1990,[4] and three types of oocyte anomaly were observed in four infertile women during IVF: GV arrest, MI arrest, and the absence of oocytes. Similar cases were observed in other previous reports,[5–8] but genetic factors related to human oocyte maturation arrest were rarely investigated and largely unknown. Recently, we determined the inheritance pattern of human oocyte MI arrest (MIM: 616780) and identified *TUBB8* (MIM: 616768) mutations that are responsible for the disease.[9–11] According to our data and the data of other groups,[9,10,12] mutations in *TUBB8* account for around 30% of the individuals with oocyte MI arrest, but the genetic causes of human oocyte GV arrest remain to be elucidated, and other genetic causes of MI arrest are largely unknown.

In the present study, we identified a homozygous mutation in *PATL2* (MIM: 614661; GenBank: NM_001145112.1) in a consanguineous family affected by oocyte GV arrest and found *PATL2* biallelic mutations (GenBank: NM_001145112.1) in individuals from an additional four families with slight phenotypic variability. Together, *in vitro* and *in vivo* evidence show that biallelic mutations in *PATL2* decrease protein amounts.

In our study, all case and control individuals (women with normal fertility) were from the Shanghai Ji Ai Genetics & IVF Institute and the Ninth Hospital affiliated with Shanghai Jiao Tong University. This study was approved by the ethics committee of the Medical College of Fudan University. All immature oocytes were donated by affected individuals after they had provided written, informed consent, and control PB1 oocytes used in this study were matured *in vitro* from GV or MI oocytes. Immature oocytes from affected individuals were fixed in 2% paraformaldehyde for immunostaining, and peripheral

[1]State Key Laboratory of Genetic Engineering, Zhongshan Hospital, Institutes of Biomedical Sciences, School of Life Sciences, Fudan University, Shanghai 200032, China; [2]Guangzhou Medical University and Guangzhou Institutes of Biomedicine and Health Joint School of Life Sciences, Guangzhou Medical University, Guangzhou 511436, China; [3]Shanghai Ji Ai Genetics and IVF Institute, Obstetrics and Gynecology Hospital, Fudan University, Shanghai 200011, China; [4]Reproductive Medicine Center, Shanghai Ninth Hospital, Shanghai Jiao Tong University, Shanghai 200011, China; [5]Key Laboratory for the Genetics of Developmental and Neuropsychiatric Disorders, Bio-X Center, Ministry of Education, Shanghai Jiao Tong University, Shanghai 200030, China; [6]Lin He's Academician Workstation of New Medicine and Clinical Translation at the Third Affiliated Hospital, Guangzhou Medical University, Guangzhou 510150, China
[7]These authors contributed equally to this work
*Correspondence: sangqing@fudan.edu.cn (Q.S.), wangleiwanglei@fudan.edu.cn (L.W.)
http://dx.doi.org/10.1016/j.ajhg.2017.08.018.

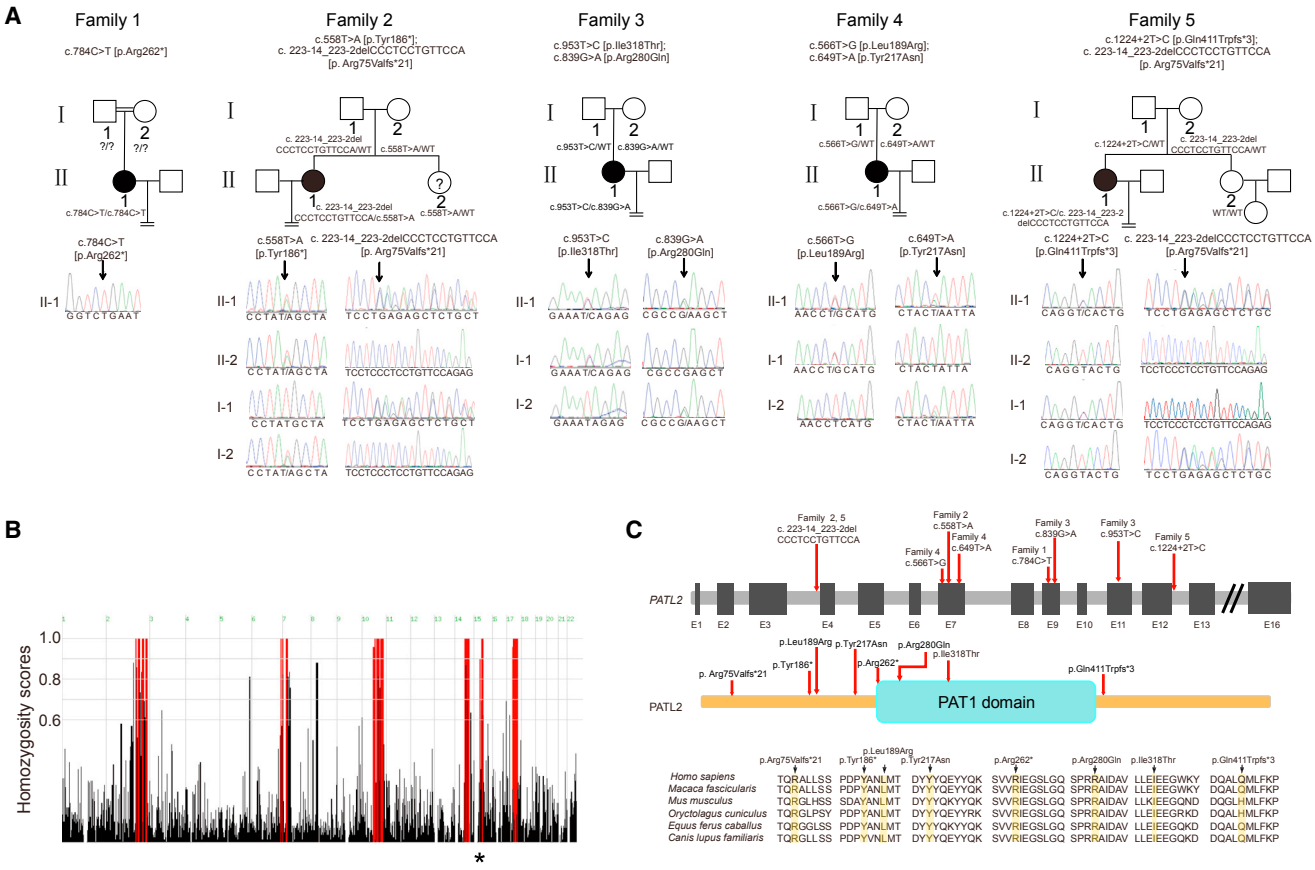

Figure 1. Identification of Mutations in *PATL2*

(A) Five pedigrees affected by oocyte maturation arrest. All five affected individuals have biallelic mutations with a recessive inheritance pattern. The proband from family 1 (with consanguineous parents) has a homozygous nonsense mutation in *PATL2*. The other individuals from families 2–5 carry compound-heterozygous variants derived from both parents. Sanger sequencing confirmation is shown below the pedigrees. Equal signs indicate infertility, and the double line between individuals I-1 and I-2 in family 1 indicates consanguinity. Black circles represent the proband. In family 2, the sister of the affected individual carrying a heterozygous mutation was not married, and her fertility was unknown.

(B) Homozygosity mapping of individual II-1 in family 1. Homozygous regions harboring the strongest signal are indicated in red. The asterisk indicates the area where *PATL2* is located.

(C) Locations and conservation of mutations in *PATL2*. The positions of all mutations are indicated in the genomic structure of *PATL2*. The affected amino acids were compared among six mammalian species in a conservation analysis.

blood was sampled for DNA extraction and sequencing according to the instructions of the QIAGEN DNA extraction kit.

We first recruited an individual diagnosed with primary infertility from a consanguineous family (family 1; Figure 1A). According to the description reported by the individual, almost all the oocytes retrieved in previous IVF and ICSI cycles performed in other provincial hospitals several years ago were arrested at the GV stage. Her latest ICSI operation produced five oocytes, of which four were arrested at the GV stage and one was arrested at the MI stage, whereas no PB1 oocytes were obtained (Table 1). Thus, the phenotype of this individual was GV arrest. After whole-exome capture (Agilent) and Illumina sequencing, the subsequent bioinformatics analysis was based on standard protocols.[13–15] The functional impact of all variants and indels was assessed by SIFT and PolyPhen-2. Because of her parental consanguinity, a recessive inheritance model was applied for the genetic analysis of homozygosity mapping with HomozygosityMapper (Figure 1B).[16] Variants were prioritized according to the following filtering criteria: (1) homozygous variants with a minor allele frequency $< 0.1\%$ in the ExAC Browser and located within the homozygous regions greater than 2.0 Mb, (2) loss-of-function alleles and damaging missense variants predicted by SIFT or PolyPhen-2, and (3) variants with high gene expression (fragments per kilobase of transcript per million mapped reads > 50) both in human and mouse oocytes according to our in-house RNA sequencing data. The intersection of the criteria led us to identify *PATL2* containing the homozygous nonsense mutation c.784C>T (p.Arg262*) (GenBank: NM_001145112.1). Subsequently, we performed mutation screening for *PATL2* by using Sanger sequencing in a cohort of 179 infertile individuals with normal menstrual cycles and hormone levels. Most of their oocytes failed to mature after repeated IVF and

Table 1. Clinical Characteristics of Affected Individuals and Their Retrieved Oocytes

Family	Age (Years)	Duration of Infertility (Years)	IVF and ICSI Cycles	Total No. of Oocytes Retrieved	GV Oocytes	MI Oocytes	PB1 Oocytes	Oocytes with Abnormal Morphology	Fertilized Oocytes	No. of Embryos That Could Be Cleaved	Embryos Arrested at an Early Stage
1	31	8	1	5	4	1	0	0	0	0	0
2	32	9	1	3	2	0	1	0	0	0	0
3	31	11	8	64	4	7	49	4	10	4	3
4	30	6	3	75	13	14	18	30	5	2	1
5	33	3	3	47	18	2	21	6	10	9	6

Abbreviations are as follows: GV, germinal vesicle; MI, metaphase I; and PB1, first polar body.

ICSI attempts. Unexpectedly, biallelic mutations in *PATL2* were detected in another four individuals in families 2–5 (Figure 1A).

Family 2 carried biallelic mutations c.558T>A (p.Tyr186*) and c. 223−14_223−2delCCCTCCTGTTCCA (p.Arg75Valfs*21). Family 3 carried compound-heterozygous missense mutations c.953T>C (p.Ile318Thr) and c.839G>A (p.Arg280Gln), whereas family 4 carried c.649T>A (p.Tyr217Asn) and c.566T>G (p.Leu189Arg). Family 5 carried compound-heterozygous splicing mutations c.1224+2T>C (p.Gln411Trpfs*3) and c.223−14_223−2delCCCTCCTGTTCCA (p.Arg75Valfs*21) (Table 2). The multiple-sequence alignment program Clustal Omega indicates that the amino acids altered in these affected individuals are highly conserved among mammalian species (Figure 1C). Clinical information of these individuals is summarized in Table 1 and Figure 2A, and full descriptions are in the Supplemental Note. In brief, the individual in family 2 had a phenotype similar to that of the family 1 proband, whereas the phenotypes of the individuals in families 3–5 were somewhat different. Apart from oocytes arrested at the GV and MI stages, some PB1 oocytes could be retrieved from individuals in families 3–5. Some of these PB1 oocytes were abnormal with a large polar body (Figure 2A), and most of the PB1 oocytes either failed to be fertilized or were fertilized but led to embryo arrest at an early stage (Table 1). These findings indicate that mutations in *PATL2* result in phenotype variability, including GV arrest, MI arrest, fertilization failure, and early embryonic arrest.

Next, to examine the genetic load of *PATL2*, we used Fisher's exact test to perform a gene burden test between the ExAC Browser (variants with a minor allele frequency below 0.1%) and the case cohort. There were ten loss-of-function or damaging missense variants in our cohort of 180 infertile individuals, and we identified 110 loss-of-function or damaging missense variants in 60,706 individuals in the ExAC Browser ($p = 3.9e{-}12$, odds ratio = 31.5). These results strongly support the genetic contribution of *PATL2* to oocyte maturation arrest.

To determine the spatial expression of *PATL2* at the mRNA level, we measured cDNAs of human oocytes and different tissues by real-time PCR analysis. Total RNA from different tissues and from GV, MI, and PB1 oocytes was extracted with an RNeasy Mini Kit (QIAGEN). Reverse transcription was performed with the PrimeScript RT Reagent Kit after the removal of genomic DNA with the gDNA Eraser (Takara). The expression level of *PATL2* was determined with specific primers (Table S1) and was normalized to the expression level of an internal *GAPDH* (MIM: 138400) control. Real-time qPCR was performed in triplicate on a 7900HT Fast Real-Time PCR System (Applied Biosystems). The relative expression level was $2^{-\Delta Ct}$, where ΔCt = Ct (*PATL2*) − Ct (*GAPDH*). We found that *PATL2* was more highly and specifically expressed in human GV, MI, and PB1 oocytes than in various kinds of somatic tissues (Figure S1A). To further confirm the amounts of PATL2 in oocytes of different stages, we used normal GV, MI, and PB1 oocytes for immunostaining as previously described.[11] We found that PATL2 was widely distributed in the cytoplasm of normal human GV oocytes and was gradually degraded in the cytoplasm of human MI and PB1 oocytes, as indicated by reduced fluorescence intensity (Figure 2B). These results indicate that PATL2 might play an important role in the process of human oocyte maturation and early embryonic development.

We next assessed the amounts of PATL2 with missense variants *in vitro* and transfected wild-type and mutant *PATL2* constructs into HeLa cells. The *PATL2* product was cloned into the pCMV6-Entry vector with a FLAG tag (Origene) after AsiSI and MluI (New England Biolabs) dual-enzyme digestion. All clones were validated by sequencing. We performed site-directed mutagenesis to introduce six variants—c.784C>T (p.Arg262*), c.558T>A (p.Tyr186*), c.953T>C (p.Ile318Thr), c.839G>A (p.Arg280Gln), c.649T>A (p.Tyr217Asn), and c.566T>G (p.Leu189Arg)—into the pCMV6-Entry vector with the KOD-Plus Mutagenesis Kit (Toyobo Life Science). HeLa cells were harvested 36 hr after transfection and washed three times with cold PBS. Total protein was extracted with RIPA lysis buffer (Shanghai Wei AO Biological Technology) and then subjected to centrifugation at 14,000 × *g* at 4°C for 30 min to yield the supernatant. Protein amounts were probed

Table 2. Overview of the *PATL2* Mutations Observed in the Five Families

Family	Genomic Position on Chr15 (bp)	cDNA Change	Protein Change	Mutation Type	SIFT[a]	PPH2[a]	1KG_eas[b]	ExAC_eas[b]
1	44,962,067	c.784C>T	p.Arg262*	stop gain	T	NA	NA	NA
2	44,966,430–44,966,442	c. 223−14_223−2delCCCTCCTGTTCCA	p. Arg75Valfs*21	splicing	NA	NA	NA	0.0017
	44,964,312	c.558T>A	p.Tyr186*	stop gain	T	NA	NA	NA
3	44,961,589	c.953T>C	p.Ile318Thr	missense	D	P	NA	NA
	44,962,012	c.839G>A	p.Arg280Gln	missense	T	D	NA	NA
4	44,964,221	c.649T>A	p.Tyr217Asn	missense	D	D	NA	NA
	44,964,304	c.566T>G	p.Leu189Arg	missense	D	D	NA	NA
5	44,966,430–44,966,442	c. 223−14_223−2delCCCTCCTGTTCCA	p. Arg75Valfs*21	splicing	NA	NA	NA	0.0017
	44,961,176	c.1224+2T>C	p.Gln411Trpfs*3	splicing	NA	NA	NA	NA

[a]Mutation assessment by SIFT and PolyPhen-2 (PPH2). T, tolerance; D, damaging; and P, probably damaging.
[b]Frequency of corresponding mutations in East Asian population of 1000 Genomes (1KG) and ExAC Browser. NA, not available.

with rabbit anti-flag (1:3,000 dilution; Sigma) and mouse anti-vinculin (1:5,000 dilution; Sigma) primary antibodies. As indicated in Figure S1B, compared with the amount of wild-type PATL2, the amount of mutant c.649T>A (p.Tyr217Asn) and c.566T>G (p.Leu189Arg) (family 4) was not obviously changed. However, the amount of mutant c.953T>C (p.Ile318Thr) (family 3) was significantly lower than that of the wild-type. Both mutant c.784C>T (p.Arg262*) (family 1) and mutant c.558T>A (p.Tyr186*) (family 2) led to the predicted premature-termination products.

To detect the effect of mutations on the amount of PATL2 in affected individuals, we used fixed oocytes from the individuals for PATL2 immunostaining. PATL2 was completely absent in oocytes from family 2, demonstrating the loss-of-function variant of PATL2 in family 2 (Figure 2B). Similarly, the oocytes from families 4 and 5 showed extremely lower amounts of PATL2 than did normal oocytes, which might be the result of protein degradation caused by the corresponding mutations (Figure 2B). These results further support the conclusion that the mutant PATL2 might be subject to more rapid degradation in our affected individuals. In addition, although mutations in family 4 had no detectable effects on the amount of PATL2 in HeLa cells (Figure S1B), the overall amount of PATL2 decreased significantly in the oocytes of the affected individual from family 4. This could be explained by faster protein degradation by *PATL2* mutations in human oocytes than in cultured cell lines.

To investigate the effects of splicing mutations on mRNA integrity *in vivo*, we sequenced *PATL2* cDNA from granulosa cells of the affected individual from family 5 by using TA-clone libraries with the specific primers shown in Table S1. We found two kinds of splicing alterations due to the mutations that were not found in the control individual. As shown in Figure 3A, a 49-bp intronic sequence before exon 4 was inserted, whereas in Figure 3B a 43-bp intronic sequence after exon 12 was retained and triggered exon skipping. Both of the splicing mutations (c.223−14_223−2delCCCTCCTGTTCCA [p.Arg75Valfs*21] and c.1224+2T>C [p.Gln411Trpfs*3]) resulted in a frameshift and protein truncation. TA-clone sequencing showed that the proportion of positive c.223−14_223−2delCCCTCCTGTTCCA (p.Arg75Valfs*21) clones (6.7% [1/15]) was lower than that of c.1224+2T>C (p.Gln411Trpfs*3) (30% [9/30]), implying that the former was affected more severely by nonsense-mediated decay than the latter.

In this study, we have identified biallelic mutations in *PATL2* in five infertile female individuals from five independent families affected by oocyte maturation arrest. We also provide evidence for the mutational effects on the amount of PATL2 *in vitro* and its localization in affected individuals' oocytes. Thus, we have uncovered an important role for *PATL2* mutations in human oocyte maturation arrest and female infertility. We found phenotypic variability in individuals with *PATL2* mutations, most likely because the different mutations have different types of effects. The function of PATL2 in the individuals from families 1 and 2 was expected to be totally lost as a result of the nonsense mutations, the phenotype of which was mainly GV arrest. As for the compound-heterozygous missense mutations in the individuals from families 3 and 4, the function of PATL2 was less severely impaired than in families 1 and 2. Correspondingly, small numbers of PB1 oocytes, in addition to GV and MI oocytes, could be retrieved from the individuals in families 3 and 4. However, either these PB1 oocytes failed to be fertilized or they were fertilized but the ensuing embryos showed early developmental arrest. We therefore infer that phenotypic variability depends on the extent of impaired function of PATL2, and greater impairment

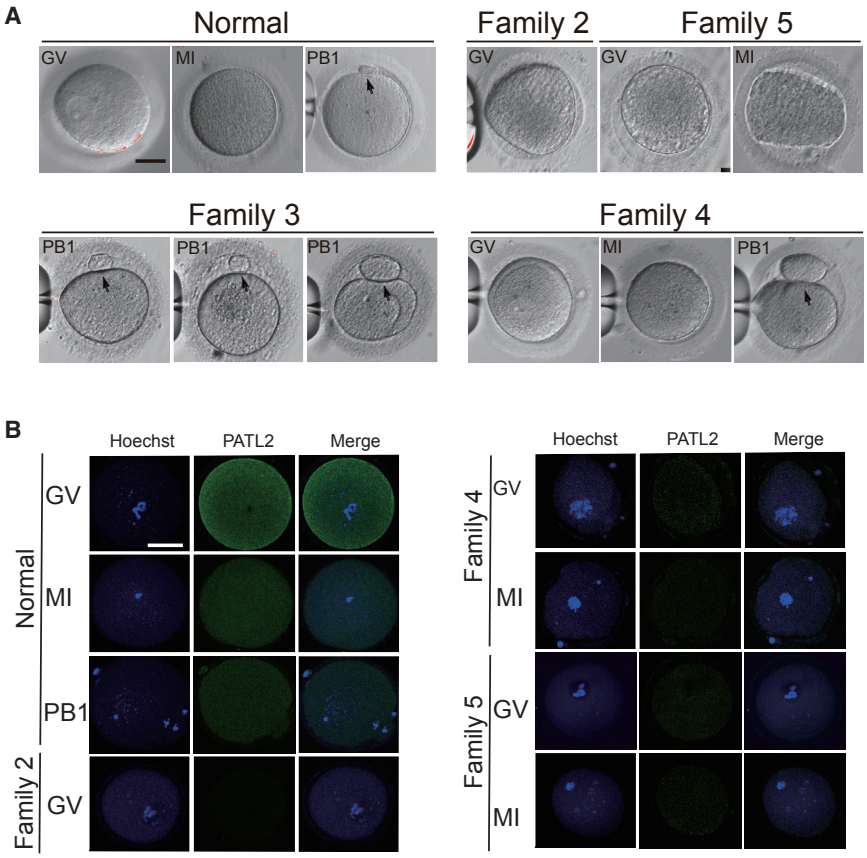

Figure 2. Phenotypes of Oocytes Retrieved from Affected Individuals

(A) The morphology of normal and affected individuals' germinal vesicle (GV), metaphase I (MI), and first polar body (PB1) oocytes. Individuals from families 3 and 4 had some PB1 oocytes, but these had abnormal PB1s, as indicated by the arrows. The scale bar represents 50 μm.

(B) Immunolabeling of normal and affected individuals' oocytes at different stages. Oocytes were immunolabeled with antibodies against PATL2 (shown in green) for visualization of the protein distribution and were counterstained with Hoechst 33342 (shown in blue) for DNA visualization. The morphologies of the oocytes were examined with an inverted microscope system (OLYMPUS IX71), and the immunolabeling was examined by confocal microscopy (Leica). PATL2 was mostly located in the cytoplasm of normal oocytes and gradually degraded during oocyte maturation. The affected individuals' oocytes showed lower fluorescence than the normal oocytes, implying that the amount of PATL2 was greatly impaired by these mutations. The scale bar represents 50 μm.

of the amount of PATL2 results in oocyte arrest at earlier stages.

PATL2 is an ortholog of *S. cerevisiae* Pat1,[17] and PATL2 was initially regarded as an mRNA-binding protein (mRNP) associated with other mRNPs such as Xp54, xRAP55, and CPEB.[18,19] It has been documented that PATL2 can repress translation in oocytes and that overexpression of *PATL2* in *Xenopus* oocytes leads to oocyte maturation arrest.[19] In this study, all affected individuals have loss-of-function mutations, and the oocytes of some individuals showed decreased or absent PATL2, which implies that the mutations cause accelerated protein degradation instead of activation. This can be explained either by different pathogenic mechanisms of *PATL2* overexpression and deletion or by bidirectional effects of PATL2 in the oocyte maturation process. The

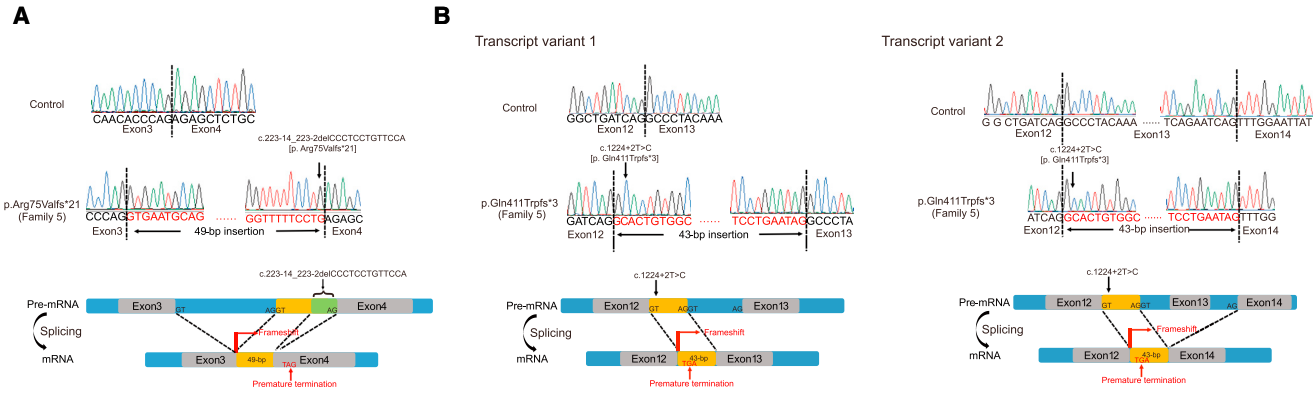

Figure 3. A Schematic Representation of the *PATL2* Splice Aberrations That Lead to Protein Truncation in Affected Individuals

(A) Schematic illustrating the effect of the *PATL2* c.223−14_223−2del CCCTCCTGTTCCA splice-site mutation. The acceptor −2A deletion disrupted the canonical acceptor splicing site and resulted in an alternative acceptor ahead of the site, causing a 49-bp insertion between exons 3 and 4.

(B) Schematic illustrating the effect of the *PATL2* c.1224+2T>C splice-site mutation. The donor +2T>C mutation missed the canonical donor splice site and made the next downstream splice site the donor site, causing a 43-bp insertion between exon 12 and exon 13 (transcript variant 1) or exon 14 (transcript variant 2). Both types of splicing mutations resulted in premature termination.

diminished PATL2 in oocytes might disrupt canonical translational repression and activate downstream transcripts for protein synthesis in an untimely manner and thus result in the observed phenotype. Thus, a possible mechanism other than loss-of-function effects is that mutations in *PATL2* might impair the amount of these mRNPs and thereby cause the phenotype. Because the function of PATL2 remains largely unknown, the exact mechanism of PATL2 in oocyte maturation should be investigated in the future.

We recently found that mutations in *TUBB8* are responsible for oocyte MI arrest and that these mutations could explain MI arrest in around 30% of affected individuals.[9–11] Here, we identified another gene, *PATL2*, associated with human oocyte maturation arrest. In clinical IVF and ICSI, the quality of oocytes and embryos is based on only morphological criteria, and the exact reasons behind recurrent IVF failure in some infertile individuals are largely unknown. Recent studies from our group and others have suggested that some human oocyte maturation arrest and early embryonic arrest follow a Mendelian inheritance pattern.[9,20,21] Thus, investigations into the genetic basis of recurrent IVF and ICSI failure might uncover additional genes and corresponding mechanisms behind oocyte and embryonic development. In addition, such investigations will provide molecular biomarkers for quality evaluation of oocytes and embryos, which will facilitate the success of IVF and ICSI procedures.

Supplemental Data

Supplemental Data include Supplemental Note, one figure, and one table and can be found with this article online at http://dx.doi.org/10.1016/j.ajhg.2017.08.018.

Acknowledgments

This work was supported by the National Key Research and Development Program of China (2017YFC1001500 and 2016YFC1000600), the National Basic Research Program of China (2015CB943300), the National Natural Science Foundation of China (81771581, 81571501, 81571397, 81571506, and 81300550), and Shanghai Rising Star Program (17QA1400200).

Received: June 28, 2017
Accepted: August 28, 2017
Published: September 28, 2017

Web Resources

1000 Genomes, http://browser.1000genomes.org
Clustal Omega, http://www.ebi.ac.uk/Tools/msa/clustalo/
dbSNP, https://www.ncbi.nlm.nih.gov/projects/SNP/
ExAC Browser, http://exac.broadinstitute.org/
GenBank, https://www.ncbi.nlm.nih.gov/genbank/
gnomAD browser, http://gnomad.broadinstitute.org/
NHLBI Exome Sequencing Project (ESP) Exome Variant Server, http://evs.gs.washington.edu/EVS/
OMIM, http://www.omim.org/
PolyPhen-2, http://genetics.bwh.harvard.edu/pph2/
RefSeq, http://www.ncbi.nlm.nih.gov/refseq/
SIFT, http://sift.bii.a-star.edu.sg/

References

1. Mehlmann, L.M. (2005). Stops and starts in mammalian oocytes: recent advances in understanding the regulation of meiotic arrest and oocyte maturation. Reproduction *130*, 791–799.
2. Eppig, J.J. (1996). Coordination of nuclear and cytoplasmic oocyte maturation in eutherian mammals. Reprod. Fertil. Dev. *8*, 485–489.
3. Dean, J. (2016). Exacting Requirements for Development of the Egg. N. Engl. J. Med. *374*, 279–280.
4. Rudak, E., Dor, J., Kimchi, M., Goldman, B., Levran, D., and Mashiach, S. (1990). Anomalies of human oocytes from infertile women undergoing treatment by in vitro fertilization. Fertil. Steril. *54*, 292–296.
5. Hartshorne, G., Montgomery, S., and Klentzeris, L. (1999). A case of failed oocyte maturation in vivo and in vitro. Fertil. Steril. *71*, 567–570.
6. Eichenlaub-Ritter, U., Schmiady, H., Kentenich, H., and Soewarto, D. (1995). Recurrent failure in polar body formation and premature chromosome condensation in oocytes from a human patient: indicators of asynchrony in nuclear and cytoplasmic maturation. Hum. Reprod. *10*, 2343–2349.
7. Bergère, M., Lombroso, R., Gombault, M., Wainer, R., and Selva, J. (2001). An idiopathic infertility with oocytes metaphase I maturation block: case report. Hum. Reprod. *16*, 2136–2138.
8. Levran, D., Farhi, J., Nahum, H., Glezerman, M., and Weissman, A. (2002). Maturation arrest of human oocytes as a cause of infertility: case report. Hum. Reprod. *17*, 1604–1609.
9. Feng, R., Sang, Q., Kuang, Y., Sun, X., Yan, Z., Zhang, S., Shi, J., Tian, G., Luchniak, A., Fukuda, Y., et al. (2016). Mutations in TUBB8 and Human Oocyte Meiotic Arrest. N. Engl. J. Med. *374*, 223–232.
10. Feng, R., Yan, Z., Li, B., Yu, M., Sang, Q., Tian, G., Xu, Y., Chen, B., Qu, R., Sun, Z., et al. (2016). Mutations in TUBB8 cause a multiplicity of phenotypes in human oocytes and early embryos. J. Med. Genet. *53*, 662–671.
11. Chen, B., Li, B., Li, D., Yan, Z., Mao, X., Xu, Y., Mu, J., Li, Q., Jin, L., He, L., et al. (2017). Novel mutations and structural deletions in TUBB8: expanding mutational and phenotypic spectrum of patients with arrest in oocyte maturation, fertilization or early embryonic development. Hum. Reprod. *32*, 457–464.
12. Huang, L., Tong, X., Luo, L., Zheng, S., Jin, R., Fu, Y., Zhou, G., Li, D., and Liu, Y. (2017). Mutation analysis of the TUBB8 gene in nine infertile women with oocyte maturation arrest. Reprod. Biomed. Online *35*, 305–310.
13. Li, H., and Durbin, R. (2009). Fast and accurate short read alignment with Burrows-Wheeler transform. Bioinformatics *25*, 1754–1760.
14. McKenna, A., Hanna, M., Banks, E., Sivachenko, A., Cibulskis, K., Kernytsky, A., Garimella, K., Altshuler, D., Gabriel, S., Daly, M., and DePristo, M.A. (2010). The Genome Analysis Toolkit: a MapReduce framework for analyzing next-generation DNA sequencing data. Genome Res. *20*, 1297–1303.

15. Wang, K., Li, M., and Hakonarson, H. (2010). ANNOVAR: functional annotation of genetic variants from high-throughput sequencing data. Nucleic Acids Res. *38*, e164.
16. Seelow, D., Schuelke, M., Hildebrandt, F., and Nürnberg, P. (2009). HomozygosityMapper–an interactive approach to homozygosity mapping. Nucleic Acids Res. *37*, W593–W599.
17. Ozgur, S., Chekulaeva, M., and Stoecklin, G. (2010). Human Pat1b connects deadenylation with mRNA decapping and controls the assembly of processing bodies. Mol. Cell. Biol. *30*, 4308–4323.
18. Radford, H.E., Meijer, H.A., and de Moor, C.H. (2008). Translational control by cytoplasmic polyadenylation in Xenopus oocytes. Biochim. Biophys. Acta *1779*, 217–229.
19. Nakamura, Y., Tanaka, K.J., Miyauchi, M., Huang, L., Tsujimoto, M., and Matsumoto, K. (2010). Translational repression by the oocyte-specific protein P100 in Xenopus. Dev. Biol. *344*, 272–283.
20. Alazami, A.M., Awad, S.M., Coskun, S., Al-Hassan, S., Hijazi, H., Abdulwahab, F.M., Poizat, C., and Alkuraya, F.S. (2015). TLE6 mutation causes the earliest known human embryonic lethality. Genome Biol. *16*, 240.
21. Xu, Y., Shi, Y., Fu, J., Yu, M., Feng, R., Sang, Q., Liang, B., Chen, B., Qu, R., Li, B., et al. (2016). Mutations in PADI6 Cause Female Infertility Characterized by Early Embryonic Arrest. Am. J. Hum. Genet. *99*, 744–752.